

Article

Modeling of Electrical Conductivity for Polymer–Carbon Nanofiber Systems

Sajad Khalil Arjmandi ¹, Jafar Khademzadeh Yeganeh ^{1,*}, Yasser Zare ²  and Kyong Yop Rhee ^{3,*} 

¹ Department of Polymer Engineering, Faculty of Engineering, Qom University of Technology, Qom 371951519, Iran

² Biomaterials and Tissue Engineering Research Group, Breast Cancer Research Center, Department of Interdisciplinary Technologies, Motamed Cancer Institute, ACECR, Tehran 1125342432, Iran

³ Department of Mechanical Engineering (BK21 Four), College of Engineering, Kyung Hee University, Yongin 17104, Korea

* Correspondence: khademzadeh@qut.ac.ir (J.K.Y.); rheekey@khu.ac.kr (K.Y.R.)

Abstract: There is not a simple model for predicting the electrical conductivity of carbon nanofiber (CNF)–polymer composites. In this manuscript, a model is proposed to predict the conductivity of CNF-filled composites. The developed model assumes the roles of CNF volume fraction, CNF dimensions, percolation onset, interphase thickness, CNF waviness, tunneling length among nanoparticles, and the fraction of the networked CNF. The outputs of the developed model correctly agree with the experimentally measured conductivity of several samples. Additionally, parametric analyses confirm the acceptable impacts of main factors on the conductivity of composites. A higher conductivity is achieved by smaller waviness and lower radius of CNFs, lower percolation onset, less tunnel distance, and higher levels of interphase depth and fraction of percolated CNFs in the nanocomposite. The maximum conductivity is obtained at 2.37 S/m by the highest volume fraction and length of CNFs.

Keywords: carbon nanofiber; polymer nanocomposites; electrical conductivity; tunneling; interphase; parametric analysis; volume fraction; percolation



Citation: Khalil Arjmandi, S.; Khademzadeh Yeganeh, J.; Zare, Y.; Rhee, K.Y. Modeling of Electrical Conductivity for Polymer–Carbon Nanofiber Systems. *Materials* **2022**, *15*, 7041. <https://doi.org/10.3390/ma15197041>

Academic Editors: M. R. M. Asyraf, Tabrej Khan, A. B. M. Supian and Agusril Syamsir

Received: 19 September 2022

Accepted: 6 October 2022

Published: 10 October 2022

Publisher's Note: MDPI stays neutral with regard to jurisdictional claims in published maps and institutional affiliations.



Copyright: © 2022 by the authors. Licensee MDPI, Basel, Switzerland. This article is an open access article distributed under the terms and conditions of the Creative Commons Attribution (CC BY) license (<https://creativecommons.org/licenses/by/4.0/>).

1. Introduction

The development of electronic technology has rapidly increased the need for materials with perfect mechanical and physical properties [1–8]. These polymer-based nanocomposites have the capability of meeting these requirements [3,6,9–18]. The use of different conductive fillers has been widely demonstrated to raise the conductivity and electrical properties. Nanocomposites are defined as a new categorized material, which consists of at least one nanoscale filler dimension [19]. Carbon nanofibers (CNFs) are favorable candidates compared to other nanoparticles with carbon structures since they possess a high aspect ratio (diameter per unit thickness) and low electrical resistivity [20–23]. Their large aspect ratio leads to producing a conductive network in polymer matrices, which changes the conductivity. The notable change in conductivity is seen at the percolation onset point due to the formation of a conductive network after percolation onset [9,24–26]. Many equations and models have been proposed in the literature to understand the network formation and conductivity of nanocomposites [27–29]. Although CNFs and carbon nanotubes (CNTs) have a close resemblance in terms of morphology and microstructure, their differences have not been widely reflected. In comparison to CNFs, CNTs are more influenced by van der Waals forces, which cause them to stay dispersed for a shorter period of time [30–32].

Electrons can be transferred between nanoparticles and the contact regions among nanofibers play an important role in electron tunneling [33,34]. In fact, a short tunneling length as the distance between two adjacent nanosheets can positively increase the conductivity of composites as a tunneling mechanism. The tunneling effect has been studied

in many papers, and can affect the electrical conductivity of CNF–polymer composites (PCNFs) [35–38]. In addition, the interphase zones between nanofillers and the polymer matrix can influence the properties of PCNFs. The impacts of interphase regions on the performances of nanocomposites have been reported in many studies [39–48]. It was reported that interphase regions can change the percolation level to smaller CNF volume fractions. In other words, the interphase depth can change the percolation onset, the conductivity, and the mechanical properties of a PCNF [29,49,50]. However, there are no models for reflecting the effects of the tunneling mechanism and the interphase zone on the conductivity of a PCNF, although these factors can contribute to higher conductivity and a smaller percolation threshold in nanocomposites.

The main advantages and novelty of this study include the applications of interphase and tunneling terms to predict the conductivity of PCNFs. The developed model considers the impacts of important factors such as tunneling distance, filler volume fraction, interphase thickness, and critical volume fraction of nanofibers (percolation onset). The roles of the tunneling region and interphase in the percolation threshold are properly indicated by the developed equations. To evaluate the proposed equations, many experimented data are applied. Additionally, the influences of various factors on the conductivity are plotted to validate the suggested equations.

2. Model Development

Percolation onset can be defined by using the aspect ratio of CNFs [51], as follows:

$$\varphi_p \approx \frac{R}{l} \quad (1)$$

where “ R ” and “ l ” are the radius and length of CNF, respectively. A layer surrounding the CNF, which is defined as interphase, should be considered in Equation (1), because the interphase layer declines the percolation and quickens the networking [52]. So, the final equation for the percolation threshold is as follows:

$$\varphi_p = \frac{15(R - 2t)}{l} \quad (2)$$

where “ t ” is interphase depth. CNFs have lengths of a few microns with diameters of around 100 nm, which results in a high aspect ratio (length/diameter > 100). The effectiveness of carbon nanofibers is decreased by the waviness of a PCNF [51]. The function of waviness can be given by assuming an equivalent length (l_{eq}) for wavy nanofibers (Figure 1), as follows:

$$u = \frac{l}{l_{eq}} \quad (3)$$

where a higher values of “ u ” exhibits further waviness, whilst $u = 1$ shows no curvature (straight nanofibers). Additionally, the electrical conduction of CNF can be decreased by curvature, which should be taken into consideration [51].

The impact of waviness on “ σ_N ”, as the natural conduction of a CNF, is expressed by:

$$\sigma_{Nw} = \frac{\sigma_N}{u} \quad (4)$$

Additionally, a CNF and its surrounding interphase express the effective nanoparticles, which are able to determine the properties and performance of CNF-based composites.

The effective volume share of a CNF can be given [33] by:

$$\varphi_{eff} = \frac{(R + t)^2(l/u + 2t)}{R^2l/u} \varphi_f \quad (5)$$

where “ φ_f ” is total volume fraction of CNFs in a PCNF.

Moreover, some nanofibers are separated in a PCNF, while the remaining ones participate in networks above the percolation threshold. The percentage of percolated CNFs, which is computed by effective filler concentration and percolation onset, is described [33] as:

$$f = \frac{\varphi_{eff}^{1/3} - \varphi_p^{1/3}}{1 - \varphi_p^{1/3}} \tag{6}$$

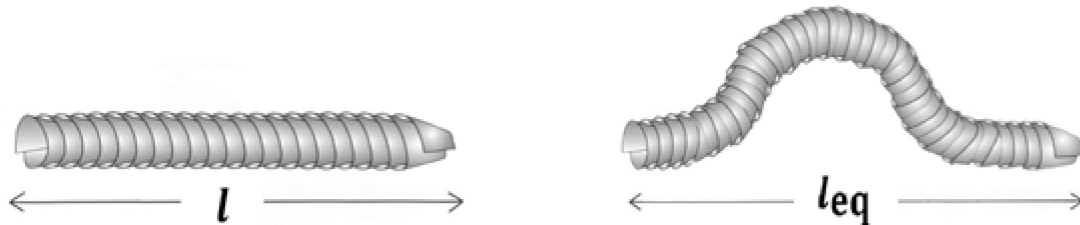


Figure 1. Straight and curved CNFs.

Deng and Zheng [53] suggested a model for conductivity of CNT-reinforced composites above percolation onset as:

$$\sigma = \sigma_0 + \frac{f\varphi_f\sigma_N}{3} \tag{7}$$

where “ σ_0 ” is electrical conductivity of polymer matrix and “ f ”, “ φ_f ”, and “ σ_N ” were defined before. However, Equation (7) is not able to reveal the impacts of tunneling and interphase in the conductivity. Using the above equations, effective filler volume fraction, waviness, and the properties of interphase and tunnels can develop Equation (7) to forecast the conductivity of a PCNF as:

$$\sigma = \frac{10^{-3} f^3 \varphi_{eff}^3 l \sigma_{Nw}}{d} \tag{8}$$

where “ d ” is the tunneling distance (Figure 2). Equation (8) expresses the electrical conductivity of a PCNF, assuming the roles of network fraction, effective volume fraction, filler conduction, and tunneling distance. Some terms, such as the oxygen functional groups, may affect the conductivity of a PCNF because it is widely known that the oxygen functional groups may reduce the electrical conductivity of CNF [54]. Additionally, the surface area resistance is effective on the conductivity [55].

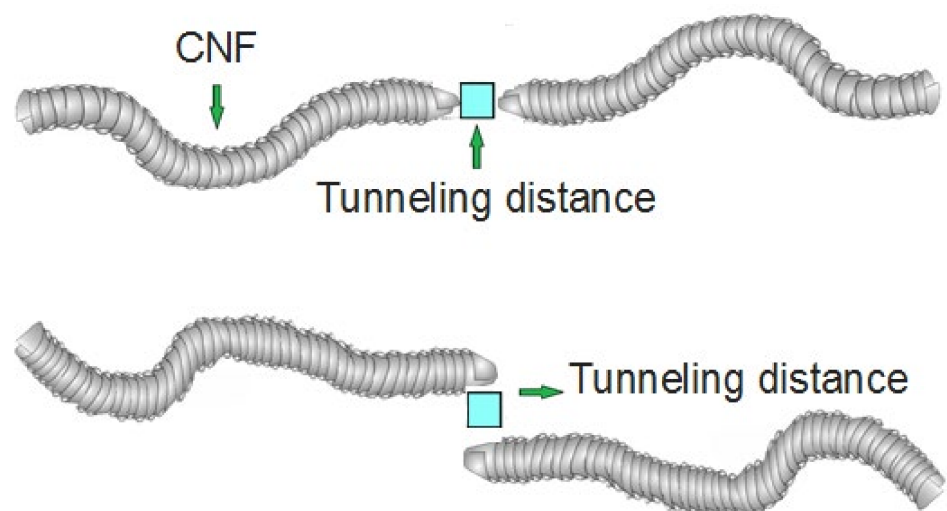


Figure 2. Placement of tunneling distance between adjacent nanofibers.

The developed equations in this paper are accurate when a CNF is randomly embedded in the polymer medium. The type of polymer medium is not important, but the random orientation of CNFs in the polymer medium is important in our model.

3. Results and Discussion

3.1. Evaluation of Parameters

The effect of each factor on the conductivity of a PCNF is surveyed by the developed model, which is reported by 2D and 3D plots. Additionally, the average levels of factors such as $R = 50$ nm, $t = 20$ nm, $l = 40$ μm , $u = 1.3$, $d = 5$ nm, $\phi_f = 0.02$, and $\sigma_N = 10^4$ S/m (on average) [56–58] are considered for all calculations.

The influences of “ ϕ_f ” and “ l ” on the conductivity are plotted in Figure 3. The higher ranges of “ ϕ_f ” and “ l ” cause the high levels of the electrical conductivity to be 2.37 S/m, whilst the lower levels of “ ϕ_f ” and “ l ” result in a lower conductivity. $\phi_f < 0.0225$ or $l < 18$ μm cause poor conductivity (near to 0). Additionally, the highest conductivity is obtained at $\phi_f = 0.04$ and $l = 100$ μm . CNFs are able to increase the electrical conductivity of nanocomposites due to their high inherent conductivity, which can reach to $\sigma_N = 10^4$ S/m. There is a big difference between the conduction of CNFs and polymers. This considerable difference is due to the higher levels of CNF conduction than those of the polymer matrix. A high number of nanofibers can create the conductive networks in PCNF, which can accelerate the charge transfer and enhance the conductivity [59–61]. Furthermore, a high CNF length increases the aspect ratio, which can optimistically control the electrical conductivity of a PCNF. Larger nanofibers can participate in the network much more easily than shorter CNFs because longer nanoparticles decline the percolation threshold, as mentioned in previous equations. In addition, longer CNFs can simplify the transfer of electrons among nanofibers and form a conductive network promoting the conductivity [62–64]. Therefore, the advanced model properly handles the impacts of CNF concentration and length on the conductivity of a PCNF.

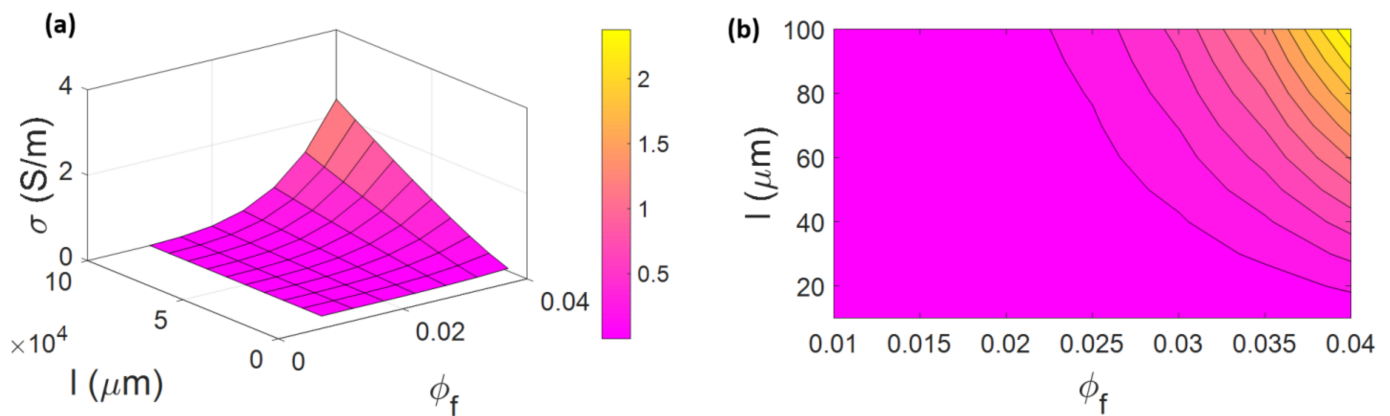


Figure 3. Impacts of “ ϕ_f ” and “ l ” on the conductivity by (a) 3D and (b) 2D diagrams.

Figure 4 shows the 3D and 2D diagrams of conductivity related to “ u ” and “ R ”. The lowest electrical conductivity of a PCNF is observed at the high levels of “ u ” and “ R ”. The maximum conductivity is achieved at 1.82 S/m at $u = 1$ and $R = 20$ nm, which means that the low values of CNF curvature and radius cause a high conductivity. Additionally, the composite is insulated at $u > 2$ and $R > 80$ nm.

CNF waviness, which is presented by “ u ”, negatively affects the effective volume fraction of nanofiber based on Equation (5). Additionally, “ u ” harmfully controls the CNF conduction, which can be seen in Equation (4). Higher levels of waviness negatively affect the effective length of nanofibers, and therefore the electrical conductivity of a PCNF. Additionally, a straight CNF causes a high range of conductivity [65,66]. Therefore, the suggested equations can properly show the effect of CNF curvature on the conductivity.

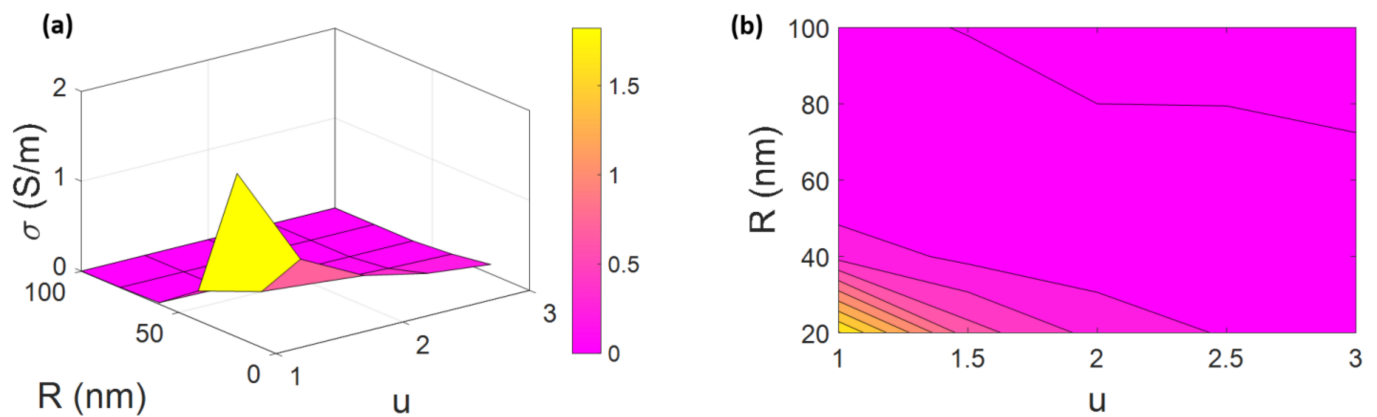


Figure 4. The stimuli of “ u ” and “ R ” on the conductivity by (a) 3D and (b) 2D designs.

Thin nanofibers positively influence the percolation onset, effective volume fraction of CNFs, and the percentage of percolated CNFs based on Equations (2), (5), and (6), respectively. The lower values of CNF radius decrease the percolation onset, increase the effective volume fraction of CNFs, and increase the percentage of percolated CNFs, which results in the enhancement of conductivity. Furthermore, thicker nanofibers are not able to increase the aspect ratio and the effectiveness of CNFs, indicating that they cannot quicken the networking [36,67–69]. Hence, it is rational to achieve a higher conductivity by utilizing thinner CNFs, confirming the developed model.

The illustrations of the electrical conductivity of PCNFs based on “ ϕ_p ” and “ d ” are presented in Figure 5. The best results are witnessed at the lowest levels of “ ϕ_p ” and “ d ”, which is calculated as about 0.1 S/m, while the lowest conduction is acquired at the highest values of the mentioned parameters. The poor electrical conductivity at 0 is seen at $\phi_p > 0.0175$ at all ranges of tunneling distance.

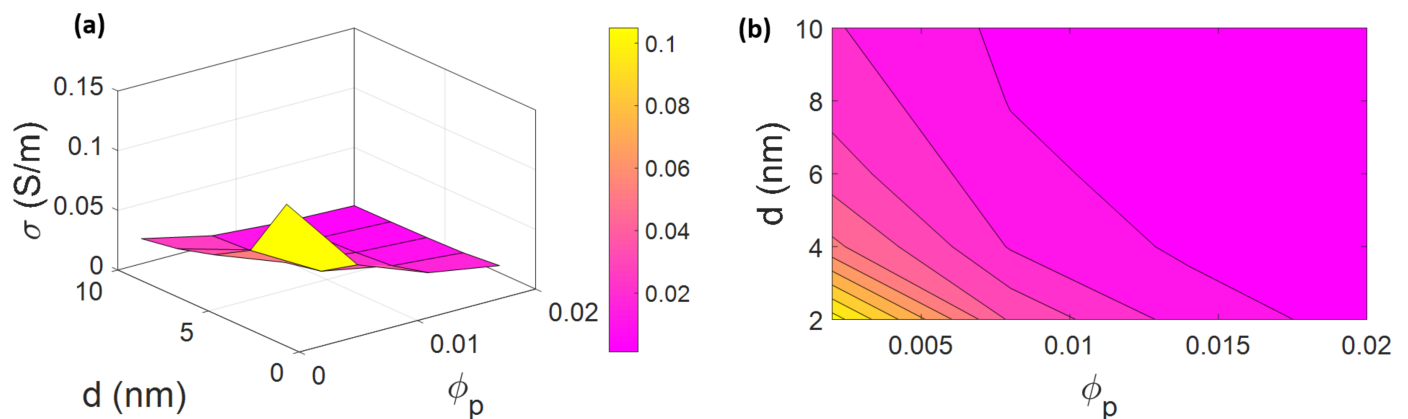


Figure 5. Theoretical conductivity by “ ϕ_p ” and “ d ”: (a) 3D and (b) contour examples.

A low percolation threshold demonstrates that nanofibers can form dense networks throughout the nanocomposites (Equation (6)) [70,71]. So, the percolation onset can play an important role in the conductivity. The minimum number of nanofibers needed for creating a contiguous network in the nanocomposites is presented as “ ϕ_p ”. The percolation onset has an opposite impact on the conductivity of composites, which has been reported in previous studies [27,72,73]. In fact, a lower level of “ ϕ_p ” can expand the CNF network, whereas the charge transfer cannot be increased by a higher value of this term. This explanation justifies the predictions of conductivity at various ranges of percolation threshold.

A separation length between nanofibers defines the tunneling distance, which manages the behavior of CNFs for percolating and networking. The electrons are transferred between

nanofibers by a tunneling effect. CNFs are capable of forming percolated networks and transferring charges when the distance between the nanofibers is lower than a critical value. In fact, a low level of tunneling distance enhances the electrical conductivity of PCNFs, which indicates the positive influence of the tunneling effect on the conductivity [35,36,74]. However, a longer tunneling distance leads to poorer transference of electrons or insulation, verifying the calculations.

The variations of conductivity by different levels of " ϕ_{eff} " and " σ_N " are indicated in Figure 6. The best conductivity is obtained by the highest ranges of " ϕ_{eff} " and " σ_N ", whilst the low levels of electrical conductivity are detected by the lowest values of these parameters. The highest conductivity for PCNF is acquired as 0.027 S/m by $\phi_{eff} = 0.04$, whilst $\phi_{eff} < 0.028$ leads to poor conductivity near to 0, which shows that CNF's effective volume share has a significant effect on the conductivity.

" ϕ_{eff} " controls the electrical conductivity of PCNFs and higher levels of this parameter increase the conductivity because it shows the positive participation of interphases and CNFs in the networks. Additionally, long and thin CNFs and thick interphases cause a high level of CNF effective volume share based on Equation (5). In addition, a high level of " ϕ_{eff} " increases the " f ", which is seen in Equation (6). In other words, higher ranges of CNF effective volume share raise the fraction of networked nanoparticles, which directly affects the electrical conductivity [62,75,76]. Although high " ϕ_{eff} " raises the conductivity, the " σ_N " factor is not able to affect the conductivity. In fact, CNF effective volume share directly handles the conductivity, but CNF conduction cannot manipulate it. The nature conduction of CNFs alone manages the conductivity of PCNFs when a high volume fraction of CNFs is used in polymer matrices, because the conductivity of polymer matrices is much lower than the conductivity of CNFs. Therefore, the direct relation between CNF conduction and the conductivity of PCNFs is logical. Additionally, it should be noted that the conductivity of CNFs is primarily based on waviness, defects, and size of nanofibers [77]. Conclusively, providing straight, long, and thin CNFs is important. However, very high levels of CNF conductivity remove its influence on the conductivity of PCNFs, confirming the advanced model.

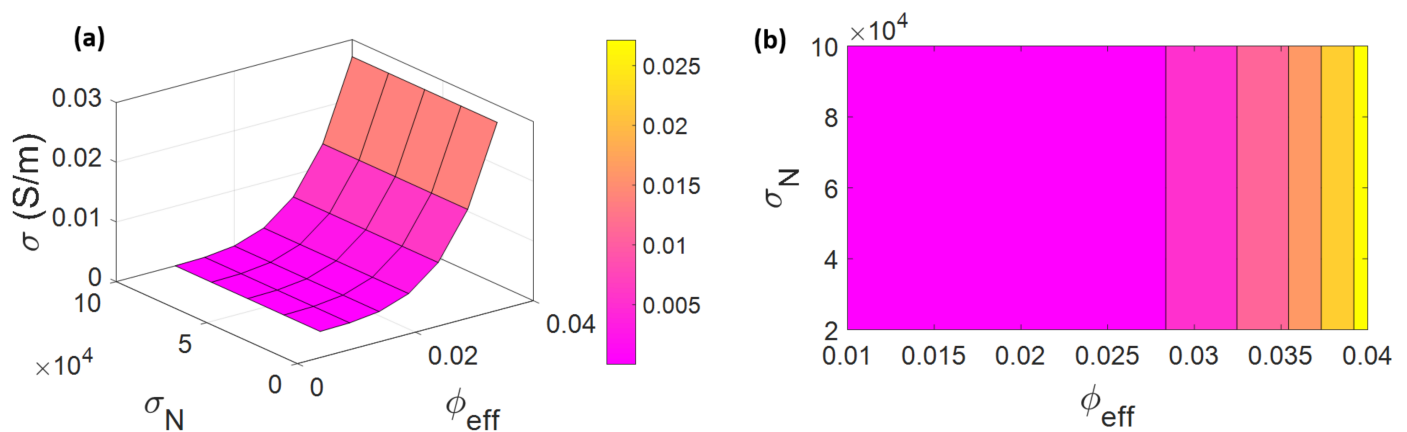


Figure 6. (a) Three-dimensional and (b) two-dimensional plots for the conductivity at various levels of " ϕ_{eff} " and " σ_N ".

Figure 7 illustrates the conductivity at different series of " t " and " f ". The best results of conductivity are achieved by the highest ranges of " t " and " f ", while the worst conduction is witnessed by the lowest levels of these terms. The highest and the lowest conductivities are estimated as 0.18 S/m ($t = 20$ nm and $f = 0.4$) and 0 ($f < 0.19$ at all ranges of t), respectively. Therefore, the effects of these factors on the conductivity are important, and the high values of interphase depth and network portion produce more conductivity.

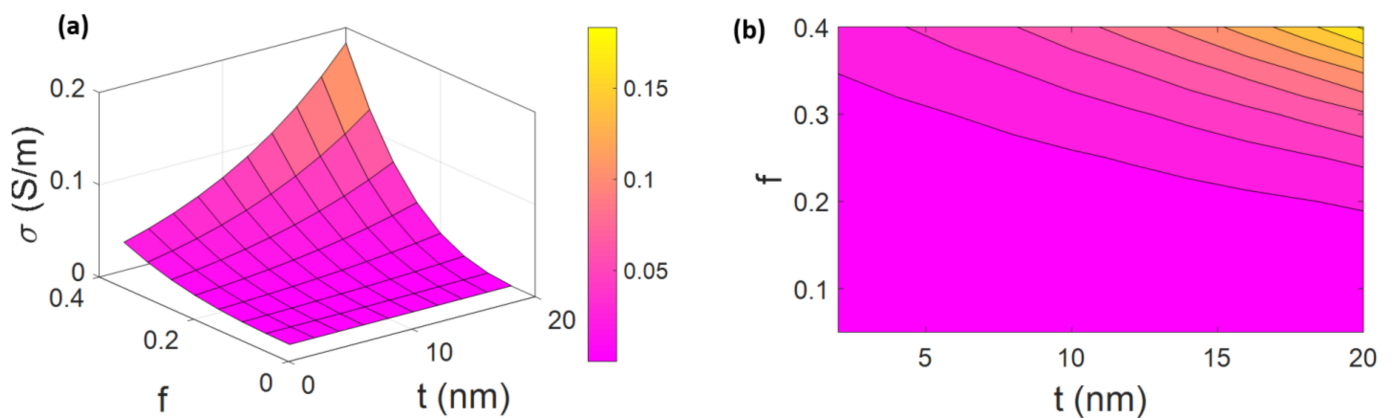


Figure 7. The relations of “ t ” and “ f ” with the conductivity by (a) 3D and (b) 2D illustrations.

As stated, an interphase layer around CNFs helps nanoparticles join to conductive nets before the actual physical links of CNFs in PCNFs. Clearly, percolated zones can be easily formed by a thick interphase. Based on Equation (2), a thicker interphase layer causes lower percolation onset, which can raise the conductivity in the composites. In other words, the interphase depth can positively influence the network by amplifying the effective CNFs [36,52,78]. In addition, perfect electron transfer needs a conductive CNF net in PCNFs. So, the density and dimensions of super-conductive nets influence the charge transfer and conduction of PCNFs. The size of contiguous conductive nets is directly shown by the fraction of percolated networks (f). An efficient electron transfer would not happen at the low levels of “ f ”, because nanofibers are not able to make a connection and nets. On the other hand, a higher “ f ” produces a denser network providing a higher conductivity. Accordingly, both interphase depth and network fraction reasonably handle the conductivity, validating the developed model.

Figure 8 shows the variations of conductivity by the mentioned factors based on the above discussion. The maximum variation of conductivity is obtained as 2.37 S/m by the volume fraction and length of CNF, while the minimum variation of conduction is achieved as 0.027 S/m by the effective volume fraction and conductivity of CNF. Additionally, optimal or desired electrical conductivity is calculated as 1.82 S/m at $u = 1$ and $R = 10$ nm, 0.1 S/m at $\varphi_p = 0.002$ and $d = 2$ nm, and 0.18 S/m at $t = 20$ nm and $f = 0.4$. Based on these descriptions, CNF volume fraction and CNF length have the most significant influences on the conductivity.

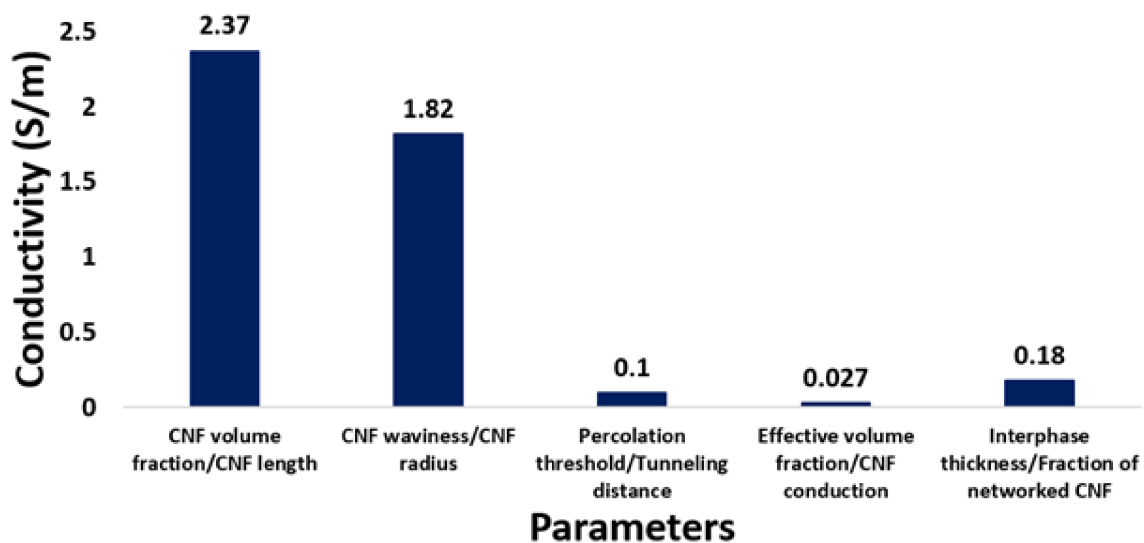


Figure 8. Variations of the calculated conductivity by different series of parameters.

3.2. Model Proofing by Experimented Data

The validity of the advised model can be confirmed by the experimented results. The agreement of calculated and experimental results is demonstrated in Figure 9 for four samples. The experimental and theoretic calculations of “ φ_p ” are exhibited in Table 1. The theoretical estimations of percolation onset depict a good accordance with the experimental data, considering interphase depth in accordance with Equation (2). In addition, the thinnest interphase produces the highest level of percolation onset, whereas the smallest value of “ φ_p ” is produced by the thickest interphase around CNFs. In fact, the interphase region declines the “ φ_p ” and creates a contiguous network before the real joining of nanoparticles. Moreover, other terms such as CNF length, CNF radius, and CNF waviness can change the percolation level based on Equation (2). By comparing the suggested model to the experimented results, the tunneling distance is measured from 0.5 to 8 nm for the samples (Table 1). Conclusively, it is observed that the developed model can properly estimate the conductivity of PCNFs utilizing the experimental results and parametric analyses.

Table 1. Information of samples and theoretical and experimental values of percolation onset.

Samples	R (nm)	u	l (μm)	t (nm)	d (nm)	φ_p Exp.	φ_p Equation (2)
HDPE ¹ /CNF [79]	75	1.1	8.0	34	6.0	0.0100	0.0144
Epoxy/randomly oriented CNF [80]	67	1.1	20	30	0.5	0.0051	0.0058
PMMA ² /CNF [81]	65	1.3	100	5.0	1.0	0.0100	0.0107
HDPE/CNF [82]	75	1.2	8.0	35	8.0	0.0100	0.0113

¹: high-density polyethylene; ²: poly (methyl methacrylate).

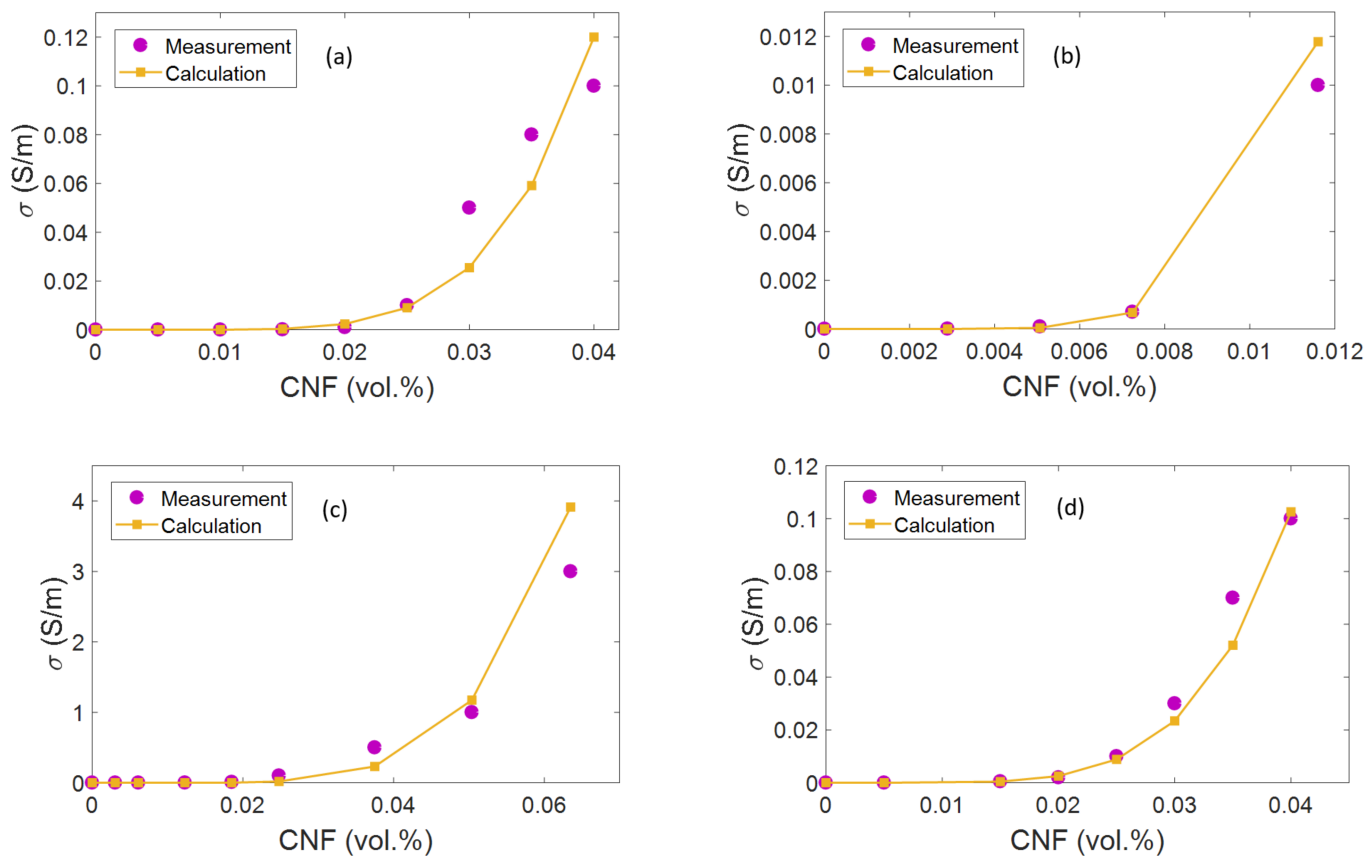


Figure 9. Agreement among theoretical and experimental data for (a) HDPE/CNF [79], (b) epoxy/randomly oriented CNF [80], (c) PMMA/CNF [81], and (d) HDPE/CNF [82] samples.

4. Conclusions

CNF waviness, filler dimensions, interphase region, effective volume fraction of filler, percolation onset, volume portion of networked CNFs, tunneling size, and CNF conduction were used to express a new methodology for the conductivity of PCNFs. The presented model showed the accurate and reasonable influences of all relevant factors on conductivity. Moreover, the experimental data of various samples agreed well with the calculations. These outcomes confirm the capability of the proposed model to forecast the conductivity of PCNFs. Conductivity is at a minimum with low levels of interphase thickness, CNF conduction, CNF radius, volume portion of percolated CNFs, effective volume fraction of CNFs, and CNF concentration, while maximum conductivity is achieved by the longest CNF lengths. Furthermore, lower percolation onset and shorter tunneling distance increase the conductivity. Additionally, the maximum conductivity is obtained as 2.37 S/m by a CNF volume fraction of 0.04 and a CNF length of 100 μm . However, effective volume fraction and conduction of CNFs have negligible impacts on the conductivity. It is stated that the high conductivity of CNFs cannot manipulate the conductivity of PCNFs.

Author Contributions: Conceptualization, J.K.Y.; Data curation, S.K.A.; Methodology, S.K.A., J.K.Y. and Y.Z.; Supervision, J.K.Y. and K.Y.R.; Validation, K.Y.R.; Visualization, K.Y.R.; Writing—original draft, Y.Z. All authors have read and agreed to the published version of the manuscript.

Funding: This work was supported by the National Research Foundation of Korea (NRF) grant funded by the Korea government (MSIT) (No. 2022M3J7A1062940).

Institutional Review Board Statement: Not applicable.

Informed Consent Statement: Not applicable.

Data Availability Statement: The data that support the findings of this study are available on request.

Conflicts of Interest: The authors declare that they have no conflicts of interest.

References

1. Mohammadpour-Haratbar, A.; Mazinani, S.; Sharif, F.; Bazargan, A.M. Improving Nonenzymatic Biosensing Performance of Electrospun Carbon Nanofibers decorated with Ni/Co Particles via Oxidation. *Appl. Biochem. Biotechnol.* **2022**, *194*, 2542–2564. [[CrossRef](#)] [[PubMed](#)]
2. Sagadevan, S.; Shahid, M.M.; Yiqiang, Z.; Oh, W.-C.; Soga, T.; Lett, J.A.; Alshahateet, S.F.; Fatimah, I.; Waqar, A.; Paiman, S. Functionalized graphene-based nanocomposites for smart optoelectronic applications. *Nanotechnol. Rev.* **2021**, *10*, 605–635. [[CrossRef](#)]
3. Bhat, A.; Budholiya, S.; Raj, S.A.; Sultan, M.T.H.; Hui, D.; Shah, A.U.M.; Safri, S.N.A. Review on nanocomposites based on aerospace applications. *Nanotechnol. Rev.* **2021**, *10*, 237–253. [[CrossRef](#)]
4. Boraie, S.B.A.; Nourmohammadi, J.; Mahdavi, F.S.; Zare, Y.; Rhee, K.Y.; Montero, A.F.; Herencia, A.J.S.; Ferrari, B. Osteogenesis capability of three-dimensionally printed poly (lactic acid)-halloysite nanotube scaffolds containing strontium ranelate. *Nanotechnol. Rev.* **2022**, *11*, 1901–1910. [[CrossRef](#)]
5. Farzaneh, A.; Rostami, A.; Nazockdast, H. Thermoplastic polyurethane/multiwalled carbon nanotubes nanocomposites: Effect of nanoparticle content, shear, and thermal processing. *Polym. Compos.* **2021**, *42*, 4804–4813. [[CrossRef](#)]
6. Tajdari, A.; Babaei, A.; Goudarzi, A.; Partovi, R.; Rostami, A. Hybridization as an efficient strategy for enhancing the performance of polymer nanocomposites. *Polym. Compos.* **2021**, *42*, 6801–6815. [[CrossRef](#)]
7. Abdollahi Boraie, S.B.; Nourmohammadi, J.; Bakhshandeh, B.; Dehghan, M.M.; Gonzalez, Z.; Ferrari, B. The effect of protelos content on the physicochemical, mechanical and biological properties of gelatin-based scaffolds. *J. Appl. Biotechnol. Rep.* **2020**, *7*, 41–47.
8. Boraie, S.B.A.; Nourmohammadi, J.; Mahdavi, F.S.; Yus, J.; Ferrandez-Montero, A.; Sanchez-Herencia, A.J.; Gonzalez, Z.; Ferrari, B. Effect of SrR delivery in the biomarkers of bone regeneration during the in vitro degradation of HNT/GN coatings prepared by EPD. *Colloids Surf. B Biointerfaces* **2020**, *190*, 110944. [[CrossRef](#)]
9. Haghgoo, M.; Ansari, R.; Hassanzadeh-Aghdam, M. Synergic effect of graphene nanoplatelets and carbon nanotubes on the electrical resistivity and percolation threshold of polymer hybrid nanocomposites. *Eur. Phys. J. Plus* **2021**, *136*, 768. [[CrossRef](#)]
10. Zare, Y.; Rhee, K.Y. Micromechanics simulation of electrical conductivity for carbon-nanotube-filled polymer system by adjusting Ouali model. *Eur. Phys. J. Plus* **2021**, *136*, 852. [[CrossRef](#)]
11. Taheri, M.; Ebrahimi, F. Buckling analysis of CFRP plates: A porosity-dependent study considering the GPLs-reinforced interphase between fiber and matrix. *Eur. Phys. J. Plus* **2020**, *135*, 1–19. [[CrossRef](#)]

12. Shahdan, D.; Chen, R.S.; Ahmad, S. Optimization of graphene nanoplatelets dispersion and nano-filler loading in bio-based polymer nanocomposites based on tensile and thermogravimetry analysis. *J. Mater. Res. Technol.* **2021**, *15*, 1284–1299. [[CrossRef](#)]
13. Ghasemi, A.R.; Soleymani, M. A new efficient buckling investigation of functionally graded CNT/fiber/polymer/metal composite panels exposed to hydrostatic pressure considering simultaneous manufacturing-induced agglomeration and imperfection issues. *Eur. Phys. J. Plus* **2021**, *136*, 1–25. [[CrossRef](#)]
14. Alshammari, A.H.; Taha, T. Structure, thermal and dielectric insights of PVC/PVP/ZnFe₂O₄ polymer nanocomposites. *Eur. Phys. J. Plus* **2021**, *136*, 1–13. [[CrossRef](#)]
15. Zare, Y.; Rhee, K.Y. Expression of normal stress difference and relaxation modulus for ternary nanocomposites containing biodegradable polymers and carbon nanotubes by storage and loss modulus data. *Compos. Part B Eng.* **2019**, *158*, 162–168. [[CrossRef](#)]
16. Zare, Y. Modeling of tensile modulus in polymer/carbon nanotubes (CNT) nanocomposites. *Synth. Met.* **2015**, *202*, 68–72. [[CrossRef](#)]
17. Zare, Y.; Garmabi, H. Nonisothermal crystallization and melting behavior of PP/nanoclay/CaCO₃ ternary nanocomposite. *J. Appl. Polym. Sci.* **2012**, *124*, 1225–1233. [[CrossRef](#)]
18. Mohammadpour-Haratbar, A.; Kiaerad, P.; Mazinani, S.; Bazargan, A.M.; Sharif, F. Bimetallic nickel–cobalt oxide nanoparticle/electrospun carbon nanofiber composites: Preparation and application for supercapacitor electrode. *Ceram. Int.* **2022**, *48*, 10015–10023. [[CrossRef](#)]
19. Jyoti, J.; Singh, B.P. A review on 3D graphene–carbon nanotube hybrid polymer nanocomposites. *J. Mater. Sci.* **2021**, *56*, 17411–17456. [[CrossRef](#)]
20. Haidyrah, A.S.; Sundaresan, P.; Venkatesh, K.; Ramaraj, S.K.; Thirumalraj, B. Fabrication of functionalized carbon nanofibers/carbon black composite for electrochemical investigation of antibacterial drug nitrofurantoin. *Colloids Surf. A Physicochem. Eng. Asp.* **2021**, *627*, 127112. [[CrossRef](#)]
21. Hosseini, S.M.; Moradi, F.; Farahani, S.K.; Bandehali, S.; Parvizian, F.; Ebrahimi, M.; Shen, J. Carbon nanofibers/chitosan nanocomposite thin film for surface modification of poly (ether sulphone) nanofiltration membrane. *Mater. Chem. Phys.* **2021**, *269*, 124720. [[CrossRef](#)]
22. Ramezani, H.; Kazemirad, S.; Shokrieh, M.; Mardanshahi, A. Effects of adding carbon nanofibers on the reduction of matrix cracking in laminated composites: Experimental and analytical approaches. *Polym. Test.* **2021**, *94*, 106988. [[CrossRef](#)]
23. Samadian, H.; Mobasheri, H.; Azami, M.; Faridi-Majidi, R. Osteoconductive and electroactive carbon nanofibers/hydroxyapatite nanocomposite tailored for bone tissue engineering: In vitro and in vivo studies. *Sci. Rep.* **2020**, *10*, 14853. [[CrossRef](#)]
24. Haghgoo, M.; Ansari, R.; Hassanzadeh-Aghdam, M.K.; Nankali, M. A novel temperature-dependent percolation model for the electrical conductivity and piezoresistive sensitivity of carbon nanotube-filled nanocomposites. *Acta Mater.* **2022**, *230*, 117870. [[CrossRef](#)]
25. Strugova, D.; Ferreira Junior, J.C.; David, É.; Demarquette, N.R. Ultra-low percolation threshold induced by thermal treatments in co-continuous blend-based PP/PS/MWCNTs nanocomposites. *Nanomaterials* **2021**, *11*, 1620. [[CrossRef](#)]
26. Mohammadpour-Haratbar, A.; Zare, Y.; Rhee, K.Y. Development of a theoretical model for estimating the electrical conductivity of a polymeric system reinforced with silver nanowires applicable for the biosensing of breast cancer cells. *J. Mater. Res. Technol.* **2022**, *18*, 4894–4902. [[CrossRef](#)]
27. Taherian, R. Experimental and analytical model for the electrical conductivity of polymer-based nanocomposites. *Compos. Sci. Technol.* **2016**, *123*, 17–31. [[CrossRef](#)]
28. Liu, Y.; He, H.; Tian, G.; Wang, Y.; Gao, J.; Wang, C.; Xu, L.; Zhang, H. Morphology evolution to form double percolation polylactide/polycaprolactone/MWCNTs nanocomposites with ultralow percolation threshold and excellent EMI shielding. *Compos. Sci. Technol.* **2021**, *214*, 108956. [[CrossRef](#)]
29. Kazemi, F.; Mohammadpour, Z.; Naghib, S.M.; Zare, Y.; Rhee, K.Y. Percolation onset and electrical conductivity for a multiphase system containing carbon nanotubes and nanoclay. *J. Mater. Res. Technol.* **2021**, *15*, 1777–1788. [[CrossRef](#)]
30. Park, J.-M.; Kim, D.-S.; Kim, S.-J.; Kim, P.-G.; Yoon, D.-J.; DeVries, K.L. Inherent sensing and interfacial evaluation of carbon nanofiber and nanotube/epoxy composites using electrical resistance measurement and micromechanical technique. *Compos. Part B Eng.* **2007**, *38*, 847–861. [[CrossRef](#)]
31. Cui, Y.; Liu, C.; Hu, S.; Yu, X. The experimental exploration of carbon nanofiber and carbon nanotube additives on thermal behavior of phase change materials. *Sol. Energy Mater. Sol. Cells* **2011**, *95*, 1208–1212. [[CrossRef](#)]
32. Parveen, S.; Rana, S.; Figueiro, R. A review on nanomaterial dispersion, microstructure, and mechanical properties of carbon nanotube and nanofiber reinforced cementitious composites. *J. Nanomater.* **2013**, *2013*, 710175. [[CrossRef](#)]
33. Feng, C.; Jiang, L. Micromechanics modeling of the electrical conductivity of carbon nanotube (CNT)–polymer nanocomposites. *Compos. Part A Appl. Sci. Manuf.* **2013**, *47*, 143–149. [[CrossRef](#)]
34. Takeda, T.; Shindo, Y.; Kuronuma, Y.; Narita, F. Modeling and characterization of the electrical conductivity of carbon nanotube-based polymer composites. *Polymer* **2011**, *52*, 3852–3856. [[CrossRef](#)]
35. Hu, N.; Karube, Y.; Yan, C.; Masuda, Z.; Fukunaga, H. Tunneling effect in a polymer/carbon nanotube nanocomposite strain sensor. *Acta Mater.* **2008**, *56*, 2929–2936. [[CrossRef](#)]
36. Zare, Y.; Rhee, K.Y. A power model to predict the electrical conductivity of CNT reinforced nanocomposites by considering interphase, networks and tunneling condition. *Compos. Part B Eng.* **2018**, *155*, 11–18. [[CrossRef](#)]

37. Kim, S.; Zare, Y.; Garmabi, H.; Rhee, K.Y. Variations of tunneling properties in poly (lactic acid)(PLA)/poly (ethylene oxide)(PEO)/carbon nanotubes (CNT) nanocomposites during hydrolytic degradation. *Sens. Actuators A Phys.* **2018**, *274*, 28–36. [[CrossRef](#)]
38. Razavi, R.; Zare, Y.; Rhee, K.Y. A two-step model for the tunneling conductivity of polymer carbon nanotube nanocomposites assuming the conduction of interphase regions. *RSC Adv.* **2017**, *7*, 50225–50233. [[CrossRef](#)]
39. Zare, Y.; Rhee, K.Y.; Park, S.-J. A modeling methodology to investigate the effect of interfacial adhesion on the yield strength of MMT reinforced nanocomposites. *J. Ind. Eng. Chem.* **2019**, *69*, 331–337. [[CrossRef](#)]
40. Zare, Y. Estimation of material and interfacial/interphase properties in clay/polymer nanocomposites by yield strength data. *Appl. Clay Sci.* **2015**, *115*, 61–66. [[CrossRef](#)]
41. Zare, Y.; Garmabi, H. Attempts to Simulate the Modulus of Polymer/Carbon Nanotube Nanocomposites and Future Trends. *Polym. Rev.* **2014**, *54*, 377–400. [[CrossRef](#)]
42. Zare, Y.; Garmabi, H. Modeling of interfacial bonding between two nanofillers (montmorillonite and CaCO₃) and a polymer matrix (PP) in a ternary polymer nanocomposite. *Appl. Surf. Sci.* **2014**, *321*, 219–225. [[CrossRef](#)]
43. Zeng, Q.; Yu, A.; Lu, G. Multiscale modeling and simulation of polymer nanocomposites. *Prog. Polym. Sci.* **2008**, *33*, 191–269. [[CrossRef](#)]
44. Boutaleb, S.; Zaïri, F.; Mesbah, A.; Nait-Abdelaziz, M.; Gloaguen, J.-M.; Boukharouba, T.; Lefebvre, J.-M. Micromechanics-based modelling of stiffness and yield stress for silica/polymer nanocomposites. *Int. J. Solids Struct.* **2009**, *46*, 1716–1726. [[CrossRef](#)]
45. Sharifzadeh, E.; Tohfegar, E.; Safajou Jahankhanemlou, M. The influences of the nanoparticles related parameters on the tensile strength of polymer nanocomposites. *Iran. J. Chem. Eng. (IJChE)* **2020**, *17*, 65–78.
46. Zare, Y. Study on interfacial properties in polymer blend ternary nanocomposites: Role of nanofiller content. *Comput. Mater. Sci.* **2016**, *111*, 334–338. [[CrossRef](#)]
47. Peng, W.; Rhim, S.; Zare, Y.; Rhee, K.Y. Effect of “Z” factor for strength of interphase layers on the tensile strength of polymer nanocomposites. *Polym. Compos.* **2019**, *40*, 1117–1122. [[CrossRef](#)]
48. Zare, Y.; Rhee, K.Y. Dependence of Z parameter for tensile strength of multi-layered interphase in polymer nanocomposites to material and interphase properties. *Nanoscale Res. Lett.* **2017**, *12*, 42. [[CrossRef](#)]
49. Shin, H.; Yang, S.; Choi, J.; Chang, S.; Cho, M. Effect of interphase percolation on mechanical behavior of nanoparticle-reinforced polymer nanocomposite with filler agglomeration: A multiscale approach. *Chem. Phys. Lett.* **2015**, *635*, 80–85. [[CrossRef](#)]
50. Zare, Y.; Rhee, K.Y. Development of Conventional Paul Model for Tensile Modulus of Polymer Carbon Nanotube Nanocomposites After Percolation Threshold by Filler Network Density. *JOM* **2020**, *72*, 4323–4329. [[CrossRef](#)]
51. Yu, Y.; Song, S.; Bu, Z.; Gu, X.; Song, G.; Sun, L. Influence of filler waviness and aspect ratio on the percolation threshold of carbon nanomaterials reinforced polymer nanocomposites. *J. Mater. Sci.* **2013**, *48*, 5727–5732. [[CrossRef](#)]
52. Choi, J.; Shin, H.; Yang, S.; Cho, M. The influence of nanoparticle size on the mechanical properties of polymer nanocomposites and the associated interphase region: A multiscale approach. *Compos. Struct.* **2015**, *119*, 365–376. [[CrossRef](#)]
53. Deng, F.; Zheng, Q.-S. An analytical model of effective electrical conductivity of carbon nanotube composites. *Appl. Phys. Lett.* **2008**, *92*, 071902. [[CrossRef](#)]
54. Chen, N.; Zhang, H.; Luo, X.-D.; Sun, C.-Y. SiO₂-decorated graphite felt electrode by silicic acid etching for iron-chromium redox flow battery. *Electrochim. Acta* **2020**, *336*, 135646. [[CrossRef](#)]
55. Zhang, H.; Tan, Y.; Luo, X.D.; Sun, C.Y.; Chen, N. Polarization Effects of a Rayon and Polyacrylonitrile Based Graphite Felt for Iron-Chromium Redox Flow Batteries. *ChemElectroChem* **2019**, *6*, 3175–3188. [[CrossRef](#)]
56. Tibbetts, G.G.; Lake, M.L.; Strong, K.L.; Rice, B.P. A review of the fabrication and properties of vapor-grown carbon nanofiber/polymer composites. *Compos. Sci. Technol.* **2007**, *67*, 1709–1718. [[CrossRef](#)]
57. Panapoy, M.; Dankeaw, A.; Ksapabutr, B. Electrical conductivity of PAN-based carbon nanofibers prepared by electrospinning method. *Thammasat Int. J. Sc. Tech* **2008**, *13*, 11–17.
58. Inagaki, M.; Yang, Y.; Kang, F. Carbon nanofibers prepared via electrospinning. *Adv. Mater.* **2012**, *24*, 2547–2566. [[CrossRef](#)]
59. Chen, P.-W.; Chung, D. Improving the electrical conductivity of composites comprised of short conducting fibers in a nonconducting matrix: The addition of a nonconducting particulate filler. *J. Electron. Mater.* **1995**, *24*, 47–51. [[CrossRef](#)]
60. Blighe, F.M.; Hernandez, Y.R.; Blau, W.J.; Coleman, J.N. Observation of Percolation-like Scaling-Far from the Percolation Threshold-in High Volume Fraction, High Conductivity Polymer-Nanotube Composite Films. *Adv. Mater.* **2007**, *19*, 4443–4447. [[CrossRef](#)]
61. Sumita, M.; Sakata, K.; Asai, S.; Miyasaka, K.; Nakagawa, H. Dispersion of fillers and the electrical conductivity of polymer blends filled with carbon black. *Polym. Bull.* **1991**, *25*, 265–271. [[CrossRef](#)]
62. Zare, Y.; Rhee, K.Y. A simple methodology to predict the tunneling conductivity of polymer/CNT nanocomposites by the roles of tunneling distance, interphase and CNT waviness. *RSC Adv.* **2017**, *7*, 34912–34921. [[CrossRef](#)]
63. Kale, S.; Sabet, F.A.; Jasiuk, I.; Ostojca-Starzewski, M. Effect of filler alignment on percolation in polymer nanocomposites using tunneling-percolation model. *J. Appl. Phys.* **2016**, *120*, 045105. [[CrossRef](#)]
64. Zhang, Y.; Li, H.; Liu, P.; Peng, Z. Study on electrical properties and thermal conductivity of carbon nanotube/epoxy resin nanocomposites with different filler aspect ratios. In Proceedings of the 2016 IEEE International Conference on High Voltage Engineering and Application (ICHVE), Chengdu, China, 19–22 September 2016; pp. 1–4.

65. Zhang, J.; Lewin, M.; Pearce, E.; Zammarano, M.; Gilman, J.W. Flame retarding polyamide 6 with melamine cyanurate and layered silicates. *Polym. Adv. Technol.* **2008**, *19*, 928–936. [[CrossRef](#)]
66. Zare, Y.; Garmabi, H.; Rhee, K.Y. Roles of filler dimensions, interphase thickness, waviness, network fraction, and tunneling distance in tunneling conductivity of polymer CNT nanocomposites. *Mater. Chem. Phys.* **2018**, *206*, 243–250. [[CrossRef](#)]
67. Crosby, A.J.; Lee, J.Y. Polymer nanocomposites: The “nano” effect on mechanical properties. *Polym. Rev.* **2007**, *47*, 217–229. [[CrossRef](#)]
68. Tessema, A.; Zhao, D.; Moll, J.; Xu, S.; Yang, R.; Li, C.; Kumar, S.K.; Kidane, A. Effect of filler loading, geometry, dispersion and temperature on thermal conductivity of polymer nanocomposites. *Polym. Test.* **2017**, *57*, 101–106. [[CrossRef](#)]
69. Mazaheri, M.; Payandehpeyman, J.; Jamasb, S. Modeling of Effective Electrical Conductivity and Percolation Behavior in Conductive-Polymer Nanocomposites Reinforced with Spherical Carbon Black. *Appl. Compos. Mater.* **2022**, *29*, 695–710. [[CrossRef](#)]
70. Kalaitzidou, K.; Fukushima, H.; Drzal, L.T. A route for polymer nanocomposites with engineered electrical conductivity and percolation threshold. *Materials* **2010**, *3*, 1089–1103. [[CrossRef](#)]
71. Tjong, S.C.; Liang, G.; Bao, S. Electrical behavior of polypropylene/multiwalled carbon nanotube nanocomposites with low percolation threshold. *Scr. Mater.* **2007**, *57*, 461–464. [[CrossRef](#)]
72. Sumita, A.; Sakata, K.; Hayakawa, Y.; Asai, S.; Miyasaka, K.; Tanemura, M. Double percolation effect on the electrical conductivity of conductive particles filled polymer blends. *Colloid Polym. Sci.* **1992**, *270*, 134–139. [[CrossRef](#)]
73. Kirkpatrick, S. Percolation and conduction. *Rev. Mod. Phys.* **1973**, *45*, 574. [[CrossRef](#)]
74. Suh, D.; Faseela, K.; Kim, W.; Park, C.; Lim, J.G.; Seo, S.; Kim, M.K.; Moon, H.; Baik, S. Electron tunneling of hierarchically structured silver nanosatellite particles for highly conductive healable nanocomposites. *Nat. Commun.* **2020**, *11*, 2252. [[CrossRef](#)]
75. Drozdov, A.D.; de Claville Christiansen, J. Modeling electrical conductivity of polymer nanocomposites with aggregated filler. *Polym. Eng. Sci.* **2020**, *60*, 1556–1565. [[CrossRef](#)]
76. Chen, B.; Evans, J.R. Nominal and effective volume fractions in polymer—Clay nanocomposites. *Macromolecules* **2006**, *39*, 1790–1796. [[CrossRef](#)]
77. Zare, Y.; Rhee, K.Y. Development of a conventional model to predict the electrical conductivity of polymer/carbon nanotubes nanocomposites by interphase, waviness and contact effects. *Compos. Part A Appl. Sci. Manuf.* **2017**, *100*, 305–312. [[CrossRef](#)]
78. Putz, K.W.; Palmeri, M.J.; Cohn, R.B.; Andrews, R.; Brinson, L.C. Effect of cross-link density on interphase creation in polymer nanocomposites. *Macromolecules* **2008**, *41*, 6752–6756. [[CrossRef](#)]
79. He, L.-X.; Tjong, S.-C. Alternating current electrical conductivity of high-density polyethylene-carbon nanofiber composites. *Eur. Phys. J. E* **2010**, *32*, 249–254. [[CrossRef](#)]
80. Ladani, R.B.; Wu, S.; Kinloch, A.J.; Ghorbani, K.; Zhang, J.; Mouritz, A.P.; Wang, C.H. Improving the toughness and electrical conductivity of epoxy nanocomposites by using aligned carbon nanofibres. *Compos. Sci. Technol.* **2015**, *117*, 146–158. [[CrossRef](#)]
81. Jimenez, G.A.; Jana, S.C. Electrically conductive polymer nanocomposites of polymethylmethacrylate and carbon nanofibers prepared by chaotic mixing. *Compos. Part A Appl. Sci. Manuf.* **2007**, *38*, 983–993. [[CrossRef](#)]
82. He, L.-X.; Tjong, S.-C. Internal field emission and conductivity relaxation in carbon nanofiber filled polymer system. *Synth. Met.* **2010**, *160*, 2085–2088. [[CrossRef](#)]